Original Research

In vitro gene expression and detergent-free reconstitution of active proteorhodopsin in lipid vesicles

Giorgio Fracasso, Yvonne Körner, David Thomas T Gonzales and T-Y. Dora Tang

Max-Planck Institute for Molecular Cell Biology and Genetics, 01307 Dresden, Germany
Corresponding author: T-Y Dora Tang. Email: tang@mpi-cbg.de

Impact statement

Our results offer the potential for straightforward, additive-free, and molecularly simple routes to building complex bioreactors based on *in vitro* transcription–translation systems and lipid vesicles.

Abstract

In situ generation of proton gradients across membranes is a key component for energy generation within cells and is therefore an important feature for the design of energy converting artificial cells. Here, we establish a stepwise method for the *in vitro* expression and detergent-free reconstitution of proteorhodopsin into the membrane of lipid vesicles. This represents a novel technique towards the bottom-up synthesis of energy-generating artificial cells.

Keywords: Lipids synthetic biology, cell-free protein expression, protein reconstitution, artificial cells, proteorhodopsin

***Experimental Biology and Medicine* 2019; 244: 314–322. DOI: 10.1177/1535370218820290**

Introduction

Cell-free synthetic biology offers powerful routes to build reaction networks from scratch. These networks can be investigated either in bulk solution or compartmentalized to generate artificial cells which mimic or replicate basic properties of natural cells. One particularly intriguing and useful reaction pathway in biology is the cell's ability to generate its own energy in the form of adenosine triphosphate (ATP), required to drive a wide range of processes within the cell. The mitochondria of eukaryotic cells and chloroplasts are examples of efficient energy conversion, where the membrane is saturated with protein complexes that drive a vectorial proton transfer process resulting in the chemiosmotic generation of ATP. Accordingly, a major goal of synthetic biology is to build artificial cells capable of energy generation inspired by biological systems.[1,2]

A key structural element of an artificial cell is either a membraneless or a membrane bound compartment which will contain and support a reaction network. Thus, some strategies for generating artificial cells are based on membraneless compartments formed via liquid–liquid phase separation and coacervation.[3–5] These compartments have the ability to passively up concentrate molecules, isolate reactions from the outer solution and separate different reaction spaces. However, the lack of membrane makes it difficult to maintain the ion gradients upon which the energy conversion process relies.[6] In comparison, synthetic membrane-bound compartments based on the spontaneous self-assembly of lipids (liposomes) and polymers (polymersomes)[3] can support electrochemical gradients across their membranes. This makes them suitable for building artificial cells capable of *de novo* energy conversion using reconstituted membrane proteins such as ATP synthase.

In pursuit of the goal of producing such artificial energy-generating cells, ATP synthase has been co-reconstituted into lipid vesicles or polymersomes with either quinone,[7] bacteriorhodopsin,[8] Bo3 oxidase,[9–11] or into glucose oxidase microcapsules.[12] Typically, these artificial organelles are activated by membrane proteins which have been purified or extracted from *in vivo* expression where the methodologies can be extremely challenging and time consuming.

In order to remedy these drawbacks, *in vitro* transcription and translation (IVTT) can offer alternative routes to membrane protein expression and reconstitution into lipid vesicles[13–16] for the synthesis of biomimetic artificial cells.[17,18] IVTT has several advantages over *in vivo* expression of proteins for the bottom-up synthesis of artificial cells due to its fast reaction times, lack of lengthy purification steps and the ability to include molecular additives if required.[19] Moreover, a broad range of membrane proteins have been successfully expressed using cell-free methods without additives (precipitation mode), with detergents

(detergent mode) or with lipid vesicles of micelles (lipid mode).[15,20–22] One example is proteorhodopsin (PR), a light-activated membrane proton pump from bacterioplankton,[23] a homologue of bacteriorhodopsin. Typically, these rhodopsins pump protons from the exterior of the cell to the interior of the cell and are proposed to be used by the cell to generate a proton-motive force for energy generation by ATP synthase. Like bacteriorhodopsin, the structure of PR is comprised of a seven-helix bundle with retinal, a chromophore, covalently bound within its center. A trans to cis configurational change in retinal occurs after light activation. This structural change leads to proton transport across the membrane, where a residue within the protein accepts a proton from retinal. In the case of PR, the proton acceptor is the ASP97 residue with a pKa of 7.7. At alkaline pHs, the residue is deprotonated and PR pumps hydrogen in the same way as bacteriorhodopsin. When Asp97 is protonated (under acid conditions), the pumping action of PR is reversed allowing PR to pump in a bidirectional manner.[24,25] Therefore, using a proton gradient to test the function of membrane associated PR relieves any issues associated with correct protein orientation. Studies have shown that the proton pumping activity of PR overexpressed in *E. coli* is sufficient to drive the formation of ATP via ATP synthase.[26] Taken together, these features make PR an ideal candidate for proton pumping within lipid vesicles as a step towards energy-generating artificial cells.

Utilizing *in vitro* bottom-up methodologies gives additional possibilities of reducing the number of molecular components required for the synthesis of artificial cells. This is particularly advantageous as any additional chemical complexity can lead to unwanted side reactions and loss of control over the incorporation of modules into the synthetic cell. Previous work relied on detergent for the *in vitro* transcription, translation, and reconstitution of PR.[27,28] However, detergents can interfere with expression and other downstream protocols in the production of artificial cells. We therefore sought to express and reconstitute active PR without the use of detergent.

Herein, we report on the use of stepwise bottom-up approaches to undertake IVTT of PR, followed by detergent-free inclusion into the lipid vesicles via a heat shock method (Figure 1). This involves three cycles of sample incubation on ice for 5 min and heat shocking at 42°C for 1 min. This methodology was adapted from heat shocking DNA into Ca^{2+}-treated competent cells[29] to destabilize the membrane and facilitate protein incorporation. As it is well known that this procedure does not affect the growth, division and replication of the cellular machinery within competent cells, we hypothesize that this treatment would not be detrimental to lipid membranes or proteins in a synthetic context. In fact, lipid vesicles will survive numerous freeze–thaw cycles between –70°C and 50°C. In addition, studies have shown that elevated temperatures have shown increased permeability to RNA while retaining lipid membrane integrity when the temperature is returned to room temperature.[30] Consequently, we show that this detergent-free methodology results in active PR within the lipid membranes. In this way, we demonstrate the viability of using a minimal *in vitro* detergent-free method as a potentially general methodology for the incorporation of membrane proteins into lipid vesicle membranes. Specifically, we used PR as a model membrane protein to demonstrate the incorporation of active proton pumps into lipid vesicle membranes with no detergent as a step towards building artificial cells capable of energy conversion.

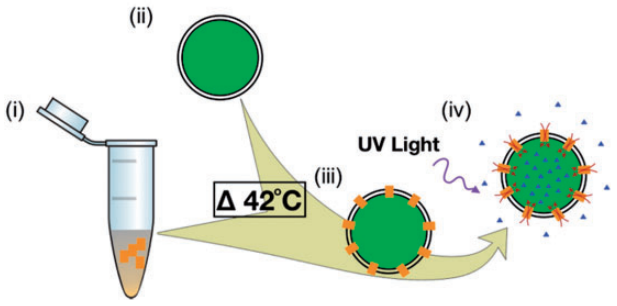

Figure 1. Schematic of the bottom-up expression and reconstitution of active proteorhodopsin into lipid vesicles: (i) proteorhodopsin is expressed using *in vitro* transcription and translation at 37°C for 4 h and then incubated with retinal at 25°C for 1 h. (ii) The reaction mixture was incubated with POPC lipid vesicles and (iii) heat shocked to incorporate proteorhodopsin into the membrane (iv) the proteoliposomes are subjected to UV light to induce proton pumping across the membrane.

Materials and methods

Materials

Phosphotidylcholine (POPC, MW= 760.1 g mol^{-1}) was purchased from Avanti-Polar lipids, Alabama, USA. Whatman® Nucleopore™ Track-Etched polycarbonate membrane filters (φ = 25 mm, pore size 20 μm), glucose (MW = 180.2 g mol^{-1}), pyranine (MW = 524.39 g mol^{-1}), all-trans retinal (MW= 284.4 g mol^{-1}), sodium dodecyl sulfate (SDS) (MW= 288.38 g mol^{-1}, bromophenol blue (MW = 669.96 g mol^{-1}), Tween 20, 1,4-dithiothreitol (DTT) (MW= 154.24 g mol^{-1}), digitonin (MW= 1229.31 g mol^{-1}) and agarose were all purchased from Sigma Aldrich, Missouri, USA. Sucrose (MW = 342.3 g mol^{-1}), Tris-HCl (MW= 157.60 g mol^{-1}), PageRuler™ Plus Prestained Protein Ladder, NuPAGE™ 4–12% Bis-Tris Gel 1.0 mm × 12 well, iBlot Gel® transfer Stacks Nitrocellulose Regular, NuPage® Running buffer (20×), NuPage® Transfer Buffer (20×), trypsin, and DH5α competent cells were purchased from Thermo Fisher Scientific, Massachusetts, USA. Glycerol 99.5% and methanol (MW = 32.04 g mol^{-1}) were purchased from VWR, Pennsylvania, USA; HEPES (MW= 238.31 g mol^{-1}) was purchased from Carl Roth, Karlsruhe, Germany, HCl (37%) and KOH (MW = 74.6 g mol^{-1}) were purchased from EMSURE, Darmstadt, Germany. RNAse inhibitor murine, Gibson Assembly® Cloning kit, XhO1 restriction enzyme with CutSmart buffer, PURExpress, Phusion high-fidelity DNA polymerase, NEBuilder HIFi DNA Assembly Master Mix were all purchased from NewEngland BioLabs, Massachusetts, USA. MaxiPrep and the QIAEX II gel extraction kit was purchased from Qiagen (NEB labs). T4 ligase and quick ligation buffer were prepared by the PEP facility at MPI-CBG, Dresden, Germany. DNA primers were custom designed and synthesized by Integrated DNA technology (IDT, Iowa, USA).

Penta-His Mouse monoclonal antibody (anti-Penta His) was purchased from Molecular Probes, Oregan, USA. Anti-GFP from Mouse $IgG_{1\kappa}$ was purchased from Roche, Basel, Switzerland, and secondary antibodies from goat anti-mouse IgG (H + L)-HRP conjugate was purchased from Biorad. ECL Western blotting detection reagents and Amersham Hyperflim ECL (GE healthcare, Chicago, USA) were imaged using a Kodak X-OMAT 2000 processor. All reagents were used without further purification, and standard kits were used as described by the manufacturer's instructions. A 384-well plate and small volume, low-base μclear Microplates were purchased from Greiner Bio-One^{TM}, Kreunsmunster, Austria.

Plasmid preparation and purification

pIVEX2.3d-PR-TEV-sfGFP was a gift from Dr. Lei Kai from MaxSynBio, MPI-Biochemistry, Martinsried. PR is from uncultured marine gamma proteobacterium (PDB code ID 2L6x). To produce pIVEX2.3d-PR (See Table 1, Supplementary Material) from pIVEX2.3d-PR-TEV-sfGFP, Xho1 restriction enzyme (NEB Biolabs) was used in conjunction with Cutsmart buffer (NEB labs) at 37°C to cut out the sfGFP sequence. The fragments were loaded on a 1× TAE 1% agarose gel and run at 120 V for 1 h. The larger DNA fragment was extracted with QIAquick Gel Extraction Kit. The gel slice was incubated at 50°C and mixed with 1 ml of isopropanol and loaded onto the spin column and centrifuged for 1 min and then further washed with washing buffer. The spin column was placed in a 1.5 ml microcentrifuge tube for the elution of DNA with water. Ligation of double-stranded DNA fragments with cohesive ends was undertaken to generate a recombinant DNA plasmid at 4°C overnight using T4 ligase (PEP facility, MPI-CBG) and quick ligation buffer (PEP facility at MPI-CBG). pIVEX2.3d-sfGFP linear fragments of double-stranded DNA was created by PCR using Phusion high-fidelity DNA polymerase (NEB labs). For a 50 µl reaction mix, 10 µl 5× Phusion HF buffer, 0.5 µM of primers (PIVEX1 EX REV with PIVEX1 FWD or PIVEX2 FWD with PIVEX2 REV (see Table 2, Supplementary Material)), 200 µM of DNTPs, and 1 unit of Phusion DNA polymerase were added. The PCR reaction was undertaken with the following parameters: 33 thermocycles of 98°C for 30 s, 54°C for 30 s to anneal and an extension step at 72°C for 1.5 min. After 33 cycles, the reaction mixture was subjected to a final extension of 5 min at 72°C. The PCR products were purified using the QIAquick PCR Purification Kit and then assembled via Gibson assembly using the NEBuilder HIFI DNA Assembly Master Mix as described by the manufacturer's instructions to generate the pIVEX2.3d-sfGFP plasmid.

All plasmid sequences were sequence verified (GATC biotech, Germany) and transformed into DH5α chemically competent cells using standard heat shock protocols as described by the manufacturer's instructions. DNA was purified from DH5α cells via MaxiPrep (Qiagen) according to the manufacturer's instructions. The concentration was determined by nanodrop and plasmids were stored in water until use.

Protein characterization

Expressed protein via *in vitro* methodologies was characterized by either fluorescence spectroscopy, UV absorbance, or via Western blot analysis. Both fluorescence and UV absorbance spectroscopy were undertaken using the Tecan Spark 20 Spectrophotometer (Tecan AG, Männedorf, Switzerland). Time-resolved fluorescence measurements of sfGFP expression was undertaken at λ_{exc} = 485 nm (bandwidth =20 nm) and λ_{emis} = 535 nm (bandwidth (20 nm) every 10 min for at least 10 h with 10 µl of reaction mixture loaded into a 384-well plate (Greiner Bio-One^{TM}). Typically, end point measurements were undertaken with 10 µl of reaction mixture which was loaded into a 384-well plate, and fluorescence spectra of sfGFP were undertaken with λ_{exc} = 480 nm (bandwidth = 15 nm) and λ_{emis} = 505 nm–650 nm (bandwidth = 5 nm)) with 1 nm step size, while UV absorbance was undertaken between 305 nm and 900 nm with a step size of 1 nm. The sample (2 µl) was loaded onto a nanoquant plate with 0.5 mm pathlength. The absorbance was normalized to 1 cm pathlength by the instrumentation software. All fluorescent spectroscopy measurements were undertaken at a fixed z position, which was determined for 10 µl of reaction mixture measured from the bottom of the well plate.

In addition, PR (MW = 23 kDa) with 6× His tag and PR-sfGFP (MW= 50 kDa) expressed from pIVEX2.3d-PR and pIVEX2.3d-PR-GFP were characterized using Western blot analysis. Typically, 10 µl of the reaction mixture was mixed with 5× loading buffer (0.44 M Tris pH 6.8, 0.5 M DTT 0.4 M SDS, 55% (by volume) glycerol, 10% bromophenol blue) and heated at 55°C for 15 min to denature the protein. Denatured protein (10 µl) and loading buffer or PageRuler^{TM} Plus Prestained Protein Ladder protein MW marker were loaded into separate channels on a pre-warmed SDS polyacrylamide gel (4–12%). The proteins were separated based on weight using a constant current and voltage (80 mAmp and 200 V) for 90 min. The gel was removed and treated with 2× transfer buffer (ThermoFisher Scientific) and methanol for 10 min. The proteins were transferred from the gel to a nitrocellulose membrane using an iBlot gel transfer device (Invitrogen iBlot dry Blotting system) and an iblot gel transfer stack at a constant current of 10 V for 20 min. The membrane was then blocked with 5wt.% skimmed milk powder in PBS-T buffer under constant shaking for 1 h at 4°C. The blocked nitrocellulose membrane was incubated with either 1× primary mouse anti-His tag (Molecular Probes) or 1× anti-GFP (Roche) overnight at 4°C with shaking. After which, excess antibody was washed from the membrane by soaking the membrane in PBS-T for 15 min and replacing the buffer three times. The membrane was then incubated with 1× secondary antibody anti-mouse (Biorad) for 1 h with shaking and then washed once with PBS-T for 15 min. Proteins with anti-His tags and anti-GFP tags were detected by chemiluminescence using the ECL Western blotting detection reagents (GE Healthcare) after incubation with 1× secondary antibody anti-mouse (Biorad) for 1 h with shaking and after washing the membrane with PBS-T for 15 min. Membranes were imaged using

Amersham Hyperflim ECL (GE healthcare) and a Kodak X-OMAT 2000 processor.

Preparation of liposomes and pyranine-containing liposomes

POPC lipid vesicles were prepared from dry lipid films, which were prepared by gentle and complete removal of chloroform from 280 µl of POPC dissolved in chloroform (32.9 mM). The dissolved lipid was loaded into a round bottomed flask by rota-evaporation (Hei-VAP AdvantageRotary Evaporators, Heidolph Instruments) at 350 atm and 130 r/min for at least 12 h. After the removal of chloroform, the lipid film was resuspended in either HEPES buffer (500 mOsmM at pH 6.2 and sucrose solution to 1100 mOsmM) or pyranine buffer (5 mM pyranine in 500 mOsmM HEPES buffer at pH 6.2 with sucrose solution to 1100 mOsmM) to a final lipid concentration of 25 mM. To maintain a constant osmolarity between all buffers, the buffers were prepared to 1100 mOsmM using a water and sucrose or glucose solution, where the osmolarity was measured using a calibrated Osmomat 3000 cryoscopic Osmometer (Gonotec, Germany). The lipid mixture was subjected to three freeze–thaw cycles in liquid nitrogen and was vortexed at maximum speed for 1 min after every cycle (IKA Vortex-Genie 2, IKA). The homogeneous lipid solution was extruded at least 11 times through a 20 µm filter using a mini extruder (Avanti polar lipids) to generate multilamellar vesicles. For pyranine-encapsulated lipid vesicles, the vesicles were washed to remove any pyranine from the outside of the vesicles via centrifugation of the lipid vesicles at 6000 × *g* for 5 min, removing the buffer and then resuspending the liposome pellet in wash buffer (500 mOsmM HEPES buffer pH 6.2 with glucose solution to 1100 mOsmM). After five wash cycles, the pellet was diluted to a known OD of 1.5 at 600 nm which was measured using absorbance spectroscopy (Nanodrop ND-100 spectrophotometer from Thermo Fisher). Lipid vesicles were imaged using confocal optical microscopy with a Zeiss LSM 880 Airy inverted (Laser Scanning Confocal, Fluorescence (Metal Halide, HXP, 120 W), Transmitted Light (Halogen), Laser Argon Multiline 488 nm, Pinhole 52.954, Objective Plan-Apochromat 63×/1.4 Oil DIC M27).

PR reconstitution and characterization of proteoliposomes

To reconstitute PR, PR-sfGFP or CALML3 was expressed using *in vitro* methodologies with and without digitonin. The cell-free reaction mixture, which had been incubated with plasmid at 37°C for 4 h and then with pyranine (5 mM) at 25°C for 1 h, was mixed with prewashed lipid vesicles (either with or without pyranine). The *in vitro* reaction mixture was mixed with the lipid vesicles at a volumetric ratio of 1:2 cell-free reaction mix:lipid vesicles. Expressed protein was incorporated into the multilamellar membrane via a heat shock method. Here, the reaction mixture and lipid vesicles were incubated on ice for 5 min, then at 42°C for 1 min and repeated three times. Control samples were prepared in the same way with IVTT reaction mixture expressing CALML3 incubated with lipid vesicles.

After heat shock, the lipid vesicles were washed by pelleting the proteoliposomes by centrifugation at 6000 × *g* for 5 min, removing the supernatant and replacing it with HEPES–glucose buffer (final 1100 mOsm, pH 6.2). After three washes, the pelleted vesicles were diluted with pyranine assay buffer (500 mOsmM of HEPES buffer made up to a final osmolarity of 1100 mOsmM with glucose solution and final pH of 8.5) to maintain a vesicle OD of 1.0.

The supernatant was reserved for analysis, and the washed proteoliposomes were characterized by UV absorbance (300–900 nm with a 1 nm step size). Background removal was undertaken by removing a spectra of liposomes which had been heat shocked in the presence of IVTT reaction mixture expressing CALM3. Fluorescence spectra of proteoliposomes containing PR-sfGFP was obtained at λ_{exc} = 480 nm (bandwidth = 15 nm), λ_{emiss} = 505 nm–650 nm (bandwidth (5 nm)).

Further analysis of the washed proteoliposomes and supernatant (1.5 ml) was undertaken by Western blot analysis. To achieve this, the proteoliposomes were pelleted by centrifugation (6000 × *g*) and all the buffer was removed. The proteoliposomes (15 µl) were incubated with loading buffer (1×), and samples were prepared for Western blot analysis as described previously.

Characterization of PR activity within lipid vesicles

Proteoliposomes-containing pyranine and either PR or CALML3 were prepared with or without heat shock methodologies or with detergent (digitonin). Each sample was typically split into two aliquots (15 µl each). The first aliquot was exposed to UV B light for 15 min using a light box and protected from any increase in temperature from the UV lamp by a cold pack, while the second aliquot was kept in the dark until measurement. Immediately after exposure to UV light, 10 µl of each aliquot was transferred to a 384-well plate (Greiner Bio-One™) and loaded a spectrometer (TECAN Spark 20 spectrophotometer, Tecan AG, Männedorf, Switzerland). PR activity in lipid vesicles was determined by measuring the emission wavelength at 514 nm (bandwidth 20 nm) after excitation at λ_{exc} = 404 nm (bandwidth 15 nm) and 454 nm (bandwidth 20 nm). All lipid vesicles had an OD of 1.0 estimated by dilution of lipid vesicles with known OD. The ratio of the peak maxima of emission at 514 nm after excitation at 454 nm and 404 nm, i.e. λ_{emis} (514 nm) @ (λ_{exc} (454)/λ_{exc} (404) nm) was determined to characterize any changes in pH after exposure to UV light and compared to the samples which had not been exposed to UV light.

The fluorescence ratio of λ_{emis} (514 nm) @ (λ_{exc} (454)/λ_{exc} (404) nm) was converted to pH units via a calibration curve of lipid vesicles containing pyranine (5 mM) at known pH values of 4.08, 4.78, 5.83, 6.21, 6.75, 7.66, 8.14. To remove pyranine from the outside of the lipid vesicles, the vesicles were washed with pyranine-free buffer at equivalent pH and osmolarity to the inside of the vesicles. The calibration curve was fit to a third-order polynomial function ($f(x) = p_1 \times x^3 + p_2 \times x^3 + p_3 \times x + p_4$ where f(x)=pH and x=λ_{emis} (514 nm) @ (λ_{exc} (454)/λ_{exc} (404) nm) (see Table 3,

Supplementary Material). The R^2 obtained from the fit was 0.9999.

Errors in the pH for the experimental data (from three repeats) were obtained by propagating the error from the polynomial fit from the calibration curve using the following equation

$$\delta y = \delta a_0 + a_1 x\left(\frac{\delta a_1}{a_1} + \frac{\delta x}{x}\right) + a_2 x^2\left(\frac{\delta a_2}{a_2} + 2\frac{\delta x}{x}\right) + a_3 x^3\left(\frac{\delta a_3}{a_3} + 3\frac{\delta x}{x}\right)$$

$$\delta \mathrm{ph} = \delta \mathrm{p4} + \mathrm{p3} \times \mathrm{pH} \times \left((\delta \mathrm{p3}/\mathrm{p3}) + (\delta \mathrm{pH}/\mathrm{pH})\right) + \mathrm{p2} \times \left(\mathrm{pH}^2\right) \times \left((\delta \mathrm{p2}/\mathrm{p2}) + 2 \times (\delta \mathrm{pH}/\mathrm{pH})\right) + \mathrm{p1} \times \left(\mathrm{pH}^3\right) \times \left((\delta \mathrm{p1}/\mathrm{p1}) + 3 \times (\delta \mathrm{pH}/\mathrm{pH})\right)$$

Differences in the pH between samples exposed to UV light and those without exposure were determined and plotted.

Trypsin treatment after cell-free expression and incubation with lipid vesicles

To remove any additional protein after heat shocking, the lipid vesicles were incubated at 25°C for 3 min with trypsin buffer (500 mOsmM HEPES buffer pH 6.2, 0.017 v/v% trypsin and glucose solution to 1100 mOsmM). After protease treatment, the lipid vesicles were washed by pelleting the proteoliposomes by centrifugation at 6000 × *g* for 5 min, removing the trypsin buffer and then resuspending the liposomes in wash buffer (500 mOsmM HEPES buffer pH 6.2 prepared to 1100 mOsmM with glucose solution) and then removing and collecting the supernatant. After three wash cycles, the pellet was diluted to a known OD of 1 which was measured using absorbance spectroscopy (at 600 nm) (Nanodrop ND-100 spectrophotometer from Thermo Fisher). The proteoliposomes were then characterized via Western blot analysis, and the activity of PR was characterized by UV absorption using TECAN Spark 20 (Tecan AG, Männedorf, Switzerland) as described previously.

Results and discussion

IVTT was undertaken with PURExpress at 37°C (see Materials and methods section), time-resolved fluorescence spectroscopy (λ_{exc} = 485 nm (bandwidth= 20 nm), λ_{em} = 535 nm (bandwidth= 20 nm)) was used to monitor IVTT of PR-sfGFP (PR-sfGFP), sfGFP (positive control) and calmodulin (CALML3) (negative control). Results showed an increase in sfGFP fluorescence for reaction mixtures containing pIVEX2.3d-sfGFP which reached a steady state after 120 min, while expression of pEXP5-NT/CALML3 (a non-fluorescent protein) and pIVEX2.3d-PR-TEV-sfGFP showed no increase in fluorescence intensity (Figure 2(a)). Additional fluorescence emission spectra of sfGFP at the end point of the experiment showed a characteristic emission profile for sfGFP with a peak maximum at 508 nm confirming that PURExpress was successful in expressing GFP from the pIVEX2.3d plasmid and that the polypeptide chain folded into its correct configuration (Figure 2(b)). The observed lack of fluorescence intensity for GFP from cell-free expressed PR-GFP could be attributed, either, to a lack of transcription or translation of pIVEX2.3d-PR-TEV-sfGFP or to incomplete folding of the polypeptide chain.

To determine whether the polypeptide chains of PR and PR-sfGFP were expressed by PURExpress, we performed a Western Blot analysis after 4 h of IVTT at 37°C, followed by incubation at 25°C with 10 μM retinal (see Materials and methods section). Western Blot analysis showed a band at approximately 23 kDa for PR (Figure 2(c), ii), at approximately 50 kDa for PR-sfGFP (Figure 2(d), i, iv) and 26 kDa for sfGFP (Figure 2(d), ii, v). The results indicate that transcription and translation of the PR-sfGFP gene were viable using PURExpress, but the polypeptide chain was unable to fold into its correct tertiary structure. This is most likely attributable to the lack of detergent in the system providing a hydrophobic environment for the correct folding of the membrane protein which then interferes with the correct folding of the fusion protein, GFP.[23,31–33]

To test whether this was the case, 0.4% w/v of digitonin was included into the cell-free reaction mix prior to the expression of sfGFP and PR-sfGFP (see Materials and methods section). Fluorescence emission spectra undertaken after 4 h of incubation showed characteristic GFP spectra for both sfGFP and PR-sfGFP (Figure 2(b)), indicating that detergent is required for correct folding of sfGFP in PR-sfGFP.[34] However, comparisons of the fluorescence spectra of sfGFP expressed with and without digitonin show more than 50% reduction in the yield of sfGFP expressed in the presence of detergent compared to without detergent (Figure 2(b) and Supplementary Figure 1). As the detergent appeared to be inhibiting cell-free protein expression by PURExpress, we sought alternative routes for folding PR after transcription and translation.

To this end, we used a heat shock methodology which included 5 min incubation of the reaction mixture with lipid vesicles (Supplementary Figure 2) on ice followed by 1 min incubation at 42°C. This was repeated three times in quick succession. End point fluorescence spectra of 1-palmitoyl-2-oleoyl-glycerol-2-phosphocholine (POPC) lipid vesicles (25 mM) which had been heat shocked in the presence of IVTT reaction mixture expressing PR-sfGFP showed characteristic fluorescence spectra from sfGFP (Figure 3(a)). These results suggest that heat shocking the reaction mixture in the presence of lipid vesicles leads to correctly folded sfGFP. As PR has no intrinsic fluorescence intensity, we attempted to characterize retinal incorporation into PR in heat-shocked lipid vesicles, where the cell-free reaction mixture was incubated with retinal (10 μM) after expression (see Materials and methods section). The results showed an increase in the absorbance spectra between 325 nm and 750 nm compared to a lipid vesicle and reaction mixture which had not been subjected to heat shock (Figure 3(b)). This increase in absorbance intensity can be attributed to the incorporation of retinal into the seven-helix bundle of PR. However, the characteristic peak of PR at 520 nm is not observed.[23] This could be attributed to low concentrations of PR or retinal or to perturbations to the retinal configuration. Despite this, the results show that the heat shock methodology in the presence of

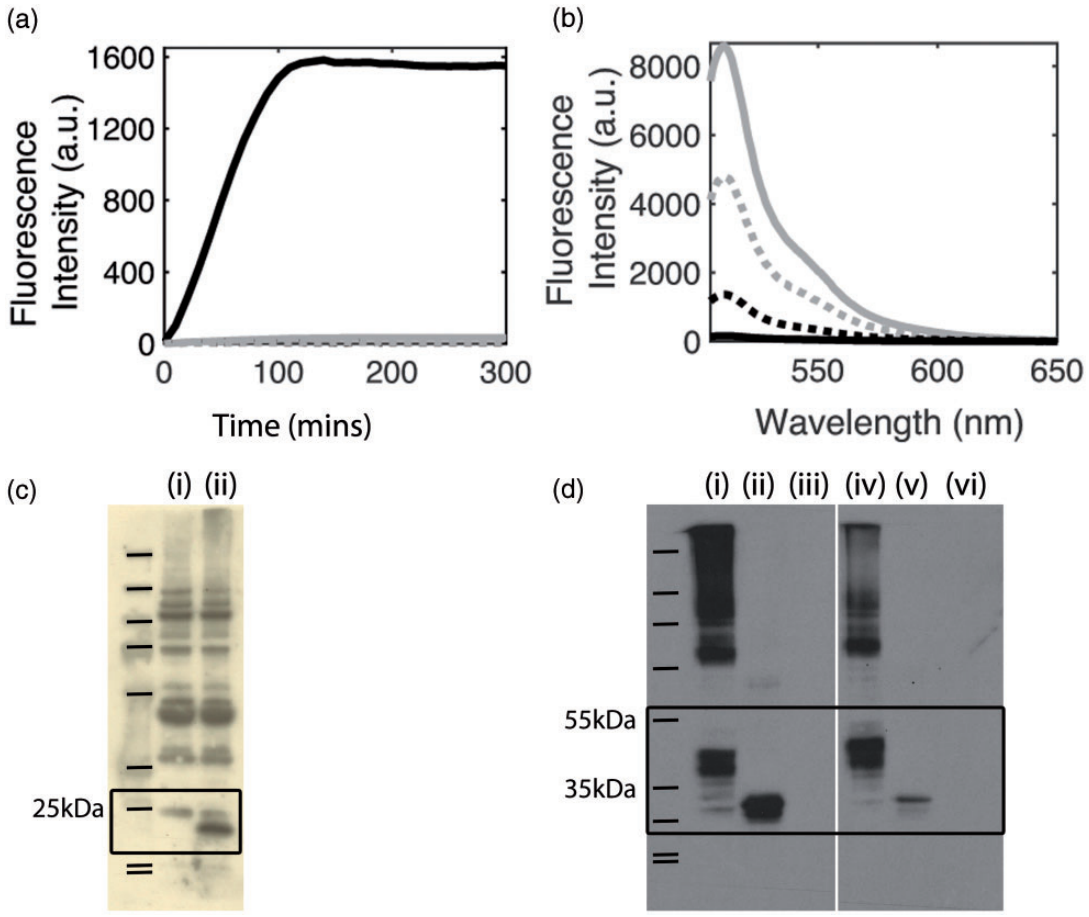

Figure 2. *In vitro* transcription translation using PURExpress at 37°C from pIVEX2.3d construct. (a) Time-resolved fluorescence spectroscopy of *in vitro* transcription and translation with PURExpress at 37°C for the expression of sfGFP (solid black line), proteorhodopsin (PR) (dotted black line), sfGFP-tagged proteorhodopsin (PR-sfGFP) (solid grey line) and a positive control calmodulin (CALML3) (dotted grey line) with $\lambda_{exc} = 485$ nm (bandwidth=20 nm) and $\lambda_{em} = 535$ nm (bandwidth = 20 nm) every 10 min. Plot shows that sfGFP reaches a steady state after 120 min with no GFP fluorescence observed from PR-sfGFP or the positive control CALML3 (b) End point fluorescence spectra of sfGFP (grey), PR-sfGFP (black) after 4 h of expression with PURExpress without digitonin for sfGFP (solid grey line) and PR-sfGFP (solid black line) and in the presence of 0.4 wt.% digitonin for sfGFP (dotted grey line) and PR-sfGFP (dotted black line) shows characteristic spectra for sfGFP. Spectra were measured with $\lambda_{exc} = 480$ nm (bandwidth = 15 nm), $\lambda_{emiss} = 505$ nm–650 nm (bandwidth (5 nm) with 1 nm step size. (c) Western blot analysis of 10 μl of *in vitro* transcription translation of calmodulin (CALM3) (i) proteorhodopsin-His tag (PR) (ii) characterized using a primary antibody anti His-tag from mouse and secondary antibody anti-mouse shows bands at approximately 25 kDa for CALML3 (i) and 23 kDa for proteorhodopsin (d) Western blot analysis from 10 μl of *in vitro* transcription translation of proteorhodopsin-sfGFP (PR-sfGFP) (i) sfGFP) (ii) or calmodulin (CALM3) (iii), PR-sfGFP diluted 1:2 with milli Q water (iv) or sfGFP diluted 1:2 with milli Q water (v) or CALM3 diluted 1:2 in milli q water (vi), using primary antibody anti His-GFP from mouse and secondary antibody anti-mouse show bands at 50 kDa and 27 kDa for PR-sfGFP and sfGFP, respectively. (A color version of this figure is available in the online journal.)

lipid vesicles leads to successful folding of sfGFP in PR-sfGFP.

We next wanted to confirm that the folded PR was associated to the membrane. Therefore, after heat shocking IVTT PR and retinal in the presence of POPC lipid vesicles, the lipid vesicles were pelleted by centrifugation, the supernatant was removed, and lipid vesicles were repeatedly washed with buffer to remove any protein which was not associated to the membrane (see Materials and methods section). Fractional Western blot analysis of the washed lipid vesicles (Figure 3(c), i) shows the presence of a band at 23 kDa corresponding to PR in the lipid membrane fraction after heat shock (Figure 3(c), i (+)). In comparison, there was no band observed at 23 kDa in the supernatant after heat shock (Figure 3(c), ii (+)) with an observed band in the supernatant with no heat shock (Figure 3(c), ii (–)). These results show that before heat shock treatment, PR was not associated with the membrane and heat shock led to increased association of the membrane protein to the lipid vesicles. While not quantitative, the results still show that IVTT PR is associated to the membrane after heat shock.

Consequently, we undertook further assays to determine whether the proton pump was active within the lipid membrane. We used an established pyranine assay[35] (see Materials and methods section) to characterize PR activity within the POPC lipid vesicle. Lipid vesicles containing pyranine (5 mM) with an internal pH of 6.2 and an external pH of 8.5 were prepared as described in the Materials and methods section. While PR will function without a pH gradient, a pH gradient was used in this study to drive unidirectional proton pumping from the outside of the vesicle to the inside. This allows robust characterization of PR activity by alleviating any issues which might arise from

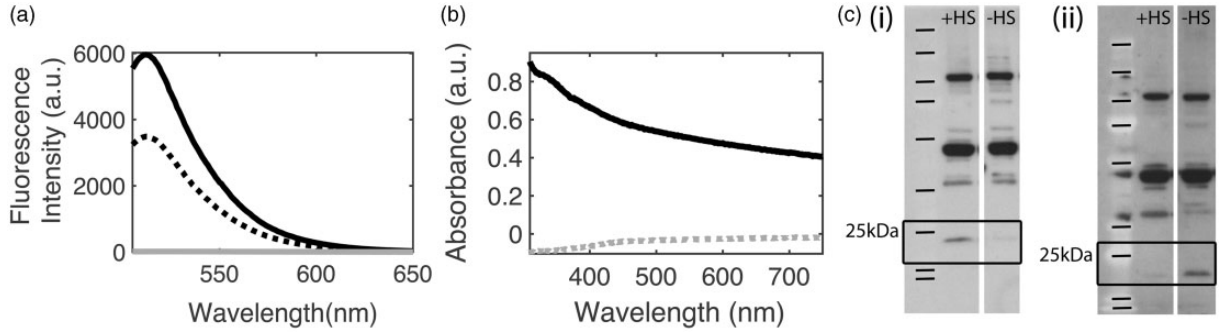

Figure 3. Proteorhodopsin folding and insertion into POPC lipid vesicles. (a) End point fluorescence spectroscopy of PR-sfGFP expressed using PURExpress at 37°C with 0.4 wt.% digitonin (dotted black line) and without digitonin (solid black line) with lipid vesicles. The *in vitro* translation/transcription reaction mixture was incubated with POPC lipid vesicles (dotted black line) or subjected to heat shock to insert the protein into the lipid vesicle (solid black line). Spectra were measured at $\lambda_{exc} = 480$ nm (bandwidth = 15 nm), $\lambda_{emiss} = 505$ nm–650 nm (bandwidth = 5 nm) with 1 nm step size show characteristic emission profiles for sfGFP indicating that a hydrophobic environment is required for the folding of sfGFP tagged to proteorhodopsin. The fluoresence spectra of only lipid vesicles are shown with the solid grey line. (b) The absorbance spectroscopy of proteorhodopsin (PR) expressed using PURExpress at 37°C measured between 310 nm and 900 nm with 1 nm step size before (dotted grey line) and after heat shock into lipid vesicles (black). An increase in absorbance intensity after heat shock can be attributed to the inclusion of retinal into a folded proteorhodopsin (c) Western blot analysis of lipid vesicles subjected to heat shock (+) and without heat shock (–) of lipid vesicles incubated with *in vitro* translation transcription reaction mix. (i) Gel of lipid vesicles washed at least five times to remove any protein not associated to the membrane increased chemiluminesence for reaction mixtures which had been subjected to heat shock (+) compared to without heatshock (–) at 23 kDa for proteorhodopsin with 6× histidine tag (ii) Western blot of the supernatant removed after pelleting lipid vesicles shock shows weak chemiluminescence without heat shock (–) compared to with heat shock (+) at 23 kDa, indicating that there is an increased of PR associated to the lipid vesicle and a decrease in the supernatant after heat shock. (A color version of this figure is available in the online journal.)

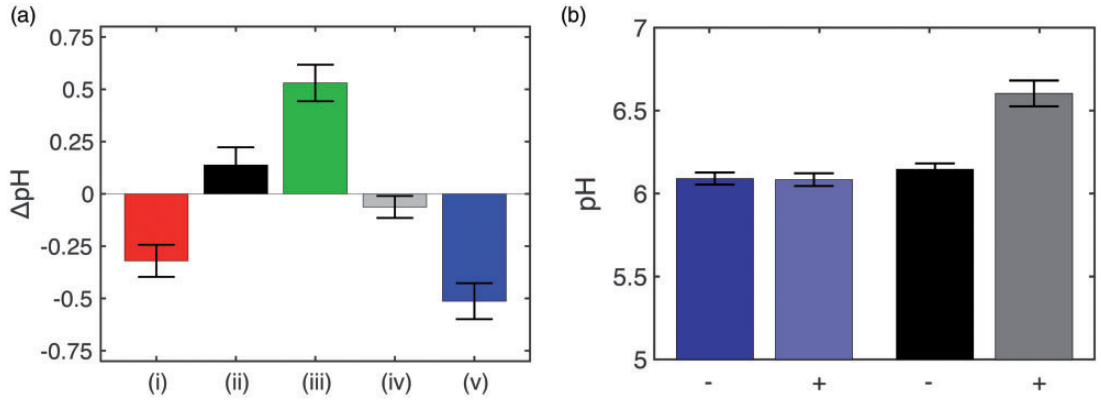

Figure 4. Proteorhodopsin activity in POPC lipid vesicles was characterized by fluorescence spectroscopic measurements of pH-sensitive pyranine dye (5 mM) in the inner lumen (pH 6.2) of multilamellar vesicles with a pH of 8.5 on the outside of the lipid vesicles. Lipid vesicles containing pyranine were either excited with UV light for 15 min (+) or kept in the dark (–). Fluorescence emission was measured by excitation at $\lambda_{exc} = 404$ nm (bandwidth 15 nm) and $\lambda_{exc} = 454$ nm (bandwidth 15 nm) and the emission measured at $\lambda_{emiss} = 514$ nm (bandwidth 20 nm). The ratio of $\lambda_{emiss} = 514$ nm from λ_{exc} (454)/λ_{exc} (404) nm was obtained and then converted to pH units via a calibration curve (Supplementary Figure 4), and the difference in the pH with and without UV radiation was determined (a) (i) proteorhodopsin expressed using PURExpress at 37°C, incubated with POPC lipid vesicles and heat shocked, $\Delta pH = -0.32 \pm 0.07$ (ii) CALML3 expressed using PURExpress at 37°C, incubated with POPC lipid vesicles and heat shocked $\Delta pH = +0.13 \pm 0.08$ (iii) proteorhodopsin (PR) expressed using PURExpress at 37°C, incubated with POPC lipid vesicles with no heat shock, $\Delta pH = +0.53 \pm 0.08$ (iv) proteorhodopsin (PR) expressed using PURExpress at 37°C with 0.4 wt.% digitonin and incubated with POPC lipid vesicles, $\Delta pH = -0.06 \pm 0.05$. (v) proteorhodopsin (PR) expressed using PURExpress at 37°C, incubated with POPC lipid vesicles, heat shocked and then incubated with trypsin (0.017 v/v %, 25°C, 3 min), $\Delta pH = -0.51 \pm 0.08$ (b) control experiments showing the effect of 15 min of UV light illumination (+) on POPC lipid vesicles filled with pyranine (5 mM) compared to storage of vesicles in the dark for 15 min (–) at (i) equal pH in the inner lumen compared to the extravesicular space (pH 6.2) and (ii) with a pH gradient across the membrane, pH 6.2 in the interlumen space and pH 8.5 on the outside of the vesicles. All measurements were undertaken on lipid vesicles and were incubated with retinal (10 μM) prior to incubation with lipid vesicles with an optical density (OD) at 600 nm of 1. Error bars are obtained from three repeats of three different experiments. (A color version of this figure is available in the online journal.)

bidirectional pumping. After heat shocking the lipid vesicles in the presence of IVTT (PR) and retinal, the proteoliposomes were subjected to 15 min of UV radiation, and the fluorescence emission at 514 nm was measured after excitation at 404 nm and 454 nm. The ratio of the pyranine fluorescence intensity at 514 nm, from λ_{exc} at 454 nm and 404 nm, was converted into pH units (Supplementary Figures 4 and 5). Using this pyranine assay, pH changes driven by UV-induced proton pumping of PR were determined. Western blot analysis confirmed that the PR was still associated with the membrane after UV treatment (Supplementary Figure 6). Our results from the pyranine assay showed that the pH change in the liposome (ΔpH) was –0.32 ± 0.07 for proteoliposomes prepared via IVTT of PR and heat shock methodologies, Δ pH = +0.13 ± 0.08 for liposomes which had been heat shocked with CALML3, and ΔpH = +0.53 ± 0.08 for liposomes which had not been subjected to heat shock in the presence of PR after 15 min of UV radiation (Figure 4(a)). The difference in ΔpH for the control experiments is most likely attributed

to variations in interactions between CALML3 and PR, where hydrophobic residues in the unfolded membrane protein PR could lead to increased membrane disruption compared to cytosolic CALML3. Further control experiments undertaken with lipid vesicles containing pyranine with no pH gradient across the membrane, showed that the UV radiation did not affect the pyranine dye (Figure 4(b)). Increase of interluminal pH is attributed to passive diffusion of protons along the proton gradient, while a decrease in pH is due to active pumping of protons against the proton gradient by PR. This pH change is comparable to previous studies in bacterial systems and with bacteriorhodopsin in polymerosomes.[8,26] Interestingly, the heat shock methodology reduced the pH in the lumen more than the detergent-based method ($\Delta pH = -0.06 \pm 0.05$) which is commensurate with increased activity via the heat shock methodology compared to the detergent-based route (Figure 4(a), iv). Furthermore, we show that proteases can be added to heat-shocked proteoliposomes, and the proteins within the membrane were protected from degradation and were still active. After pelleted and washed lipid vesicles, which had been heat shocked in the presence of IVTT PR, were subjected to mild treatment with trypsin (0.017% by volume), a band at 23 kDa corresponding to PR (supplementary Figure 7i (+HS)) was observed by Western blot analysis. In comparison, no band at 23 kDa from Western blot analysis was observed for the supernatant which had been removed from the heat-shocked lipid vesicles (supplementary Figure 7ii (+HS)). Taken together, these results show that PR which has been heat shocked into lipid vesicles are protected from mild trypsin treatment with no presence of PR in the surrounding supernatant. Moreover, pyranine assays show that the PR remains active in the membrane with a ΔpH of -0.51 ± 0.08 after protease treatment.

Conclusions

We present a simple and direct route to active membrane protein reconstitution using *in vitro* methods and detergent-free reconstitution. Our measured pH changes are comparable to other *in vitro* and *in vivo* systems as well as to detergent-based methods. Significantly, our results offer a straightforward, additive-free and molecularly simple route to building complex bioreactors based on IVTT systems. Naturally, there are questions which have surfaced from this study, for example, is this methodology applicable to other membrane proteins? Will other proteins survive the heat shock process and fold into an active state into lipid membranes? Therefore, could this methodology be used universally to reconstitute a broad range of membrane proteins? For further application in activated liposomes, one thing that would need to be addressed is the orientation of the membrane protein after insertion into the membrane. One way to ensure unified orientation could be to tag large moieties to either the N′ or C′ terminus to drive specific directional insertion. If these methodologies were used for the goal of building artificial cells capable of energy conversion, then the amount of protons produced by PR would need to be assessed for powering ATP synthase within lipid vesicles. Moreover, this methodology could be applied to more complex membrane proteins such as ATP synthase. The cell-free expression and reconstitution of ATP synthase has already been demonstrated,[36] and further work could focus on the detergent-free reconstitution of ATP synthase. Despite these open questions, the use of detergent-free, *in vitro* methodologies could simplify and expand the current synthetic biology toolbox for the generation of artificial cells from the bottom up.

Authors' contributions: TYDT conceived the project; GF, YK, DTTG undertook the experiments and data analysis; GF and TYDT discussed the results; TYDT, GF wrote the article.

ACKNOWLEDGMENTS

We thank Dr. Lei Kai for helpful discussions and for the plasmid gift (pIVEX2.3D-PR-TEV-SFGFP). We thank the Light Microscopy Facility (LMF) MPI-CBG, Mr. M. Ivankovic and Mr. L. Pastori for assistance with Western blot experiments and statistical analysis and Miss S. Shetty for discussions and undertaking preliminary experiments.

DECLARATION OF CONFLICTING INTERESTS

The author(s) declared no potential conflicts of interest with respect to the research, authorship, and/or publication of this article.

FUNDING

Funding was provided by the MaxSynBio consortium, which is jointly funded by the Federal Ministry of Education and Research of Germany and the Max Planck Society, *and* the Centre for Functional Electronic Devices, Technische Universitat Dresden funded by the DFG.

REFERENCES

1. Pohorille A, Deamer D. Artificial cells: prospects for biotechnology. *Trends Biotechnol* 2002;**20**:123–8
2. Schwille P, Spatz J, Landfester K, Bodenschatz E, Herminghaus S, Sourjik V, Erb T, Bastiaens P, Lipowsky R, Hyman A, Dabrock P, Baret J-C, Vidakovic-Koch T, Bieling P, Dimova R, Mutschler H, Robinson T, Tang T-Y D, Wegner S, Sundmacher K. MaxSynBio – avenues towards creating cells from the bottom up, *Angew. Chemie Int. Ed.*, 2018; 57:13382-13392
3. Li M, Huang X, Tang T-YD, Mann S. Synthetic cellularity based on non-lipid micro-compartments and protocell models *Curr Opin Chem Biol*, 2014; 22:1-14
4. Vieregg JR, Tang T-YD. Polynucleotides in cellular mimics: coacervates and lipid vesicles, *Curr Opin Colloid Interface Sci* 2016; 26, 50-57
5. Douliez J-P, Martin N, Gaillard C, Beneyton T, Baret J-C, Mann S, Beven L. Catanionic coacervate droplets as a surfactant-based membrane-free protocell model. *Angew Chemie Int Ed* 2017;**56**:13689–93
6. Dora Tang T-Y, Rohaida Che Hak C, Thompson AJ, Kuimova MK, Williams DS, Perriman AW, Mann S. Fatty acid membrane assembly on coacervate microdroplets as a step towards a hybrid protocell model. *Nature Chem* 2014;**6**:527–33
7. Steinberg-Yfrach G, Rigaud J-L, Durantini EN, Moore AL, Gust D, Moore TA. Light-driven production of ATP catalysed by F0F1-ATP synthase in an artificial photosynthetic membrane. *Nature* 1998;**392**:479–82

8. Choi H-J, Montemagno CD. Artificial organelle: ATP synthesis from cellular mimetic polymersomes. *Nano Lett* 2005;**5**:2538–42
9. Otrin L, Marušič N, Bednarz C, Vidaković-Koch T, Lieberwirth I, Landfester K, Sundmacher K. Toward artificial mitochondrion: mimicking oxidative phosphorylation in polymer and hybrid membranes. *Nano Lett* 2017;**17**:6816–21
10. Nilsson T, Lundin CR, Nordlund G, Ädelroth P, von Ballmoos C, Brzezinski P. Lipid-mediated protein-protein interactions modulate respiration-driven ATP synthesis. *Sci Rep* 2016;**6**:24113
11. von Ballmoos C, Biner O, Nilsson T, Brzezinski P. Mimicking respiratory phosphorylation using purified enzymes. *Biochim Biophys Acta – Bioenerg* 2016;**1857**:321–31
12. Duan L, Qi W, Yan X, He Q, Cui Y, Wang K, Li D, Li J. Proton gradients produced by glucose oxidase microcapsules containing motor F_0 F_1-ATPase for continuous ATP biosynthesis. *J Phys Chem B* 2009;**113**:395–9
13. Shinoda T, Shinya N, Ito K, Ishizuka-Katsura Y, Ohsawa N, Terada T, Hirata K, Kawano Y, Yamamoto M, Tomita T, Ishibashi Y, Hirabayashi Y, Kimura-Someya T, Shirouzu M, Yokoyama S. Cell-free methods to produce structurally intact mammalian membrane proteins. *Sci Rep* 2016;**6**:30442
14. Bernhard F, Tozawa Y. Cell-free expression – making a mark. *Curr Opin Struct Biol* 2013;**23**:374–80
15. Schwarz D, Dötsch V, Bernhard F. Production of membrane proteins using cell-free expression systems. *Proteomics* 2008;**8**:3933–46
16. Caschera F. Bacterial cell-free expression technology to in vitro systems engineering and optimization. *Synth Syst Biotechnol* 2017;**2**:97–104
17. Shin J, Noireaux V. An *E. coli* cell-free expression toolbox: application to synthetic gene circuits and artificial cells. *ACS Synth Biol* 2012;**1**:29–41
18. Noireaux V, Libchaber A. A vesicle bioreactor as a step toward an artificial cell assembly. *Proc Natl Acad Sci USA* 2004;**101**:17669 LP–74
19. Sachse R, Dondapati SK, Fenz SF, Schmidt T, Kubick S. Membrane protein synthesis in cell-free systems: from bio-mimetic systems to bio-membranes. *FEBS Lett* 2014;**588**:2774–81
20. Niwa T, Sasaki Y, Uemura E, Nakamura S, Akiyama M, Ando M, Sawada S, Mukai S, Ueda T, Taguchi H, Akiyoshi K. Comprehensive study of liposome-assisted synthesis of membrane proteins using a reconstituted cell-free translation system. *Sci Rep* 2016;**5**:18025
21. Lyukmanova EN, Shenkarev ZO, Khabibullina NF, Kopeina GS, Shulepko MA, Paramonov AS, Mineev KS, Tikhonov RV, Shingarova LN, Petrovskaya LE, Dolgikh DA, Arseniev AS, Kirpichnikov MP. Lipid-protein nanodiscs for cell-free production of integral membrane proteins in a soluble and folded state: comparison with detergent micelles, bicelles and liposomes. *Biochim Biophys Acta* 2012;1818: 349-58
22. Periasamy A, Shadiac N, Amalraj A, Garajová S, Nagarajan Y, Waters S, Mertens HDT, Hrmova M. Cell-free protein synthesis of membrane (1,3)-β-D-glucan (curdlan) synthase: co-translational insertion in liposomes and reconstitution in nanodiscs. *Biochim Biophys Acta* 2013; 1828: 743-57.
23. Gourdon P, Alfredsson A, Pedersen A, Malmerberg E, Nyblom M, Widell M, Berntsson R, Pinhassi J, Braiman M, Hansson Ö, Bonander N, Karlsson G, Neutze R. Optimized in vitro and in vivo expression of proteorhodopsin: a seven-transmembrane proton pump. *Protein Expr Purif* 2008;**58**:103–13
24. Friedrich T, Geibel S, Kalmbach R, Chizhov I, Ataka K, Heberle J, Engelhard M, Bamberg E. Proteorhodopsin is a light-driven proton pump with variable vectoriality. *J Mol Biol* 2002;**321**:821–38
25. É. Lörinczi M-K, Verhoefen J, Wachtveitl AC, Woerner C, Glaubitz M, Engelhard E, Bamberg T. Friedrich Voltage- and pH-dependent changes in vectoriality of photocurrents mediated by wild-type and mutant proteorhodopsins upon expression in Xenopus oocytes. *J Mol Biol* 2009;**393**:320–41
26. Martinez A, Bradley AS, Waldbauer JR, Summons RE, DeLong EF. Proteorhodopsin photosystem gene expression enables photophosphorylation in a heterologous host. *Proc Natl Acad Sci* 2007;**104**:5590–5
27. Reckel S, Gottstein D, Stehle J, Löhr F, Verhoefen M-K, Takeda M, Silvers R, Kainosho M, Glaubitz C, Wachtveitl J, Bernhard F, Schwalbe H, Güntert P, Dötsch V. Solution NMR structure of proteorhodopsin. *Angew Chem Int Ed Engl* 2011;**50**:11942–6
28. Klyszejko AL, Shastri S, Mari SA, Grubmüller H, Muller DJ, Glaubitz C. Folding and assembly of proteorhodopsin. *J Mol Biol* 2008;**376**:35–41
29. Froger A, Hall JE. Transformation of plasmid DNA into *E. coli* using the heat shock method. *J Vis Exp* 2007;**6**:253
30. O'Flaherty DK, Kamat NP, Mirza FN, Li L, Prywes N, Szostak JW. Copying of mixed-sequence RNA templates inside model protocells. *J Am Chem Soc* 2018;**140**:5171–8
31. Palmer E, Freeman T. Investigation into the use of C- and N-terminal GFP fusion proteins for subcellular localization studies using reverse transfection microarrays. *Comp Funct Genomics* 2004;**5**:342–53
32. Wang H, Chong S. Visualization of coupled protein folding and binding in bacteria and purification of the heterodimeric complex. *Proc Natl Acad Sci USA* 2003;**100**:478–83
33. Waldo GS, Standish BM, Berendzen J, Terwilliger TC. Rapid protein-folding assay using green fluorescent protein. *Nat Biotechnol* 1999;**17**:691–5
34. Stone KM, Voska J, Kinnebrew M, Pavlova A, Junk MJN, Han S. Structural insight into proteorhodopsin oligomers. *Biophys J* 2013;**104**:472–81
35. Amali AJ, Singh S, Rangaraj N, Patra D, Rana RK. Poly (l-Lysine)–pyranine-3 coacervate mediated nanoparticle-assembly: fabrication of dynamic pH-responsive containers. *Chem Commun* 2012;**48**:856–8
36. Matthies D, Haberstock S, Joos F, Dötsch V, Vonck J, Bernhard F, Meier T. Cell-free expression and assembly of ATP synthase. *J Mol Biol* 2011;**413**:593–603

(Received September 10, 2018, Accepted November 26, 2018)